172 (2022) 207449

Contents lists available at ScienceDirect

Micro and Nanostructures

journal homepage: www.journals.elsevier.com/micro-and-nanostructures

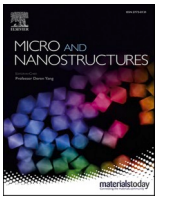

Evidence of weak strain field in InAs/GaAs submonolayer quantum dots

T.F. Cantalice [a], A. Alzeidan [a,*], G.M. Jacobsen [b], T. Borrely [a], M.D. Teodoro [b], A.A. Quivy [a]

[a] Institute of Physics, University of São Paulo, Rua do Matão 1371, 05508-090, São Paulo, SP, Brazil
[b] Departamento de Física, Universidade Federal de São Carlos, 13565-905, São Carlos, SP, Brazil

ARTICLE INFO

Keywords:
Quantum dots
Submonolayer
Segregation
Rapid thermal annealing
Photoluminescence
Surface reconstruction

ABSTRACT

We used rapid thermal annealing and low-temperature photoluminescence to compare the optoelectronic properties of InAs/GaAs Stranski-Krastanov and submonolayer quantum dots. After annealing, the former showed large changes in their optical spectra, whereas the latter remained almost insensitive and had optical properties similar to those of an InGaAs quantum well. This contrast was attributed to the presence of In segregation during the submonolayer deposition that led to strong In–Ga intermixing and hindered the formation of the submonolayer quantum dots. The optical results point out that, in such conditions, the strain field in the InAs/GaAs system is too weak to effectively provide vertical alignment of the small two-dimensional islands nucleated in consecutive InAs submonolayers. To further improve the properties of submonolayer quantum dots, segregation should be reduced and an initial (2 × 4) surface reconstruction should be preferred, as it is the only one able to provide true two-dimensional InAs islands.

1. Introduction

InAs quantum dots (QDs) have attracted much attention over the last three decades due to their high potential to improve the performance of optoelectronic devices such as lasers [1], infrared photodetectors [2], and intermediate-band solar cells [3]. The confinement of carriers along all three directions of space provides a lower threshold current in lasers and allows the operation of infrared photodetectors under normal incidence, with a lower dark current and longer relaxation times of the photoexcited carriers when compared to the same devices based on quantum wells. In intermediate-band solar cells, the discrete energy levels of QDs can extend the absorption of radiation below the bandgap of the host material and are expected to yield an overall increase in quantum efficiency.

The usual way to obtain InAs/GaAs QDs is the Stranski-Krastanov growth mode, which consists in depositing slightly more than 1.7 monolayers (MLs) of InAs material over a GaAs substrate and taking advantage of the lattice mismatch between both materials to spontaneously produce an ensemble of tiny three-dimensional (3D) InAs islands scattered all over the surface [4]. Although such Stranski-Krastanov quantum dots (SKQDs) were successfully used for decades, the own nature of the self-assembling process is also associated with some drawbacks which, nowadays, clearly limit further improvements of devices. Among them, one can cite the rather low areal density of such nanostructures (1–5 × 10^{10} cm^{-2}), their high aspect ratio (base/height), the lack of control to modify their

* Corresponding author.
E-mail address: alzeidan@if.usp.br (A. Alzeidan).

https://doi.org/10.1016/j.micrna.2022.207449
Received 3 July 2022; Received in revised form 9 November 2022; Accepted 17 November 2022
Available online 17 November 2022

size and tune their optical properties, and the presence of a wetting layer—a thin layer of InGaAs material that lies between the SKQDs and contributes to increasing the strain in the system. Several ways have been proposed to solve some of these issues, for instance, the growth of multiple layers of SKQDs [5,6] and the use of more complex structures involving confinement barriers [7], resonant tunnel barriers [8], or the insertion of QDs inside a quantum well [9]. An interesting and more disruptive method was achieved when the submonolayer technique [10] was first used to obtain a new type of quantum dot. It consists of the cycled deposition of a fraction of a monolayer of InAs—generally between 0.3 and 0.5 ML—followed by a few monolayers of GaAs. Under the right growth conditions, a very high density of narrow two-dimensional (2D) islands, as high [11] as 10^{12} cm^{-2}, can be nucleated in each InAs submonolayer deposited on the GaAs surface. Due to the strain field resulting from the lattice mismatch between both materials, one expects the small 2D islands of consecutive InAs submonolayers to nucleate on top of each other, forming thus vertical stacks that will behave as quantum dots. The total height of such nanostructures—and therefore their energy levels as well—can be easily tuned by repeating the deposition cycle as many times as necessary [12], and the deposition of only a fraction of InAs monolayer at a time results in the total absence of a wetting layer. Such submonolayer quantum dots (SMLQDs) have already been successfully used in several types of devices and provided better results when compared to the same devices fabricated with SKQDs [13–15].

However, recent structural and optoelectrical results from the literature strongly suggest that current SMLQDs may still be far from being fully optimized, as they look different from their nominal structure and are always shorter than expected, with no regular shape and no internal periodicity [11,16,17]. This is probably because they are generally grown using the well-established conditions of conventional SKQDs. Therefore, it seems to be necessary to keep optimizing their growth parameters to improve their properties. One major difficulty, though, is that most experimental techniques usually employed in the field are not of much use, as the SMLQDs are grown in a planar way and, consequently, have no measurable height, unlike SKQDs that are generally 4–7 nm high and can be easily observed by atomic force microscopy (AFM) before being covered. Since it appears that InAs/GaAs SMLQDs consist of small In-rich InGaAs agglomerates (with a size of 3–7 nm) dispersed in an InGaAs matrix [17], other experimental techniques like scanning electron microscopy (SEM), transmission electron microscopy (TEM) and x-ray diffraction (XRD) can only provide very limited information. As a consequence, it is necessary to find other techniques capable of providing valuable information about this new type of nanostructure. One indirect way to reach this goal is to perform rapid thermal annealing (RTA), which is a post-growth technique consisting in submitting the samples to a high temperature for a short time. It is known that, when applied to SKQDs, this technique leads to a strong diffusion of In atoms out of the QDs, resulting in large changes in their photoluminescence (PL) spectra that can be explained in terms of their new structural properties after the RTA process [18].

Therefore, to shed some light on the differences between SKQDs and SMLQDs and on how to improve the latter, we used RTA and PL on several samples containing different types of In(Ga)As/GaAs nanostructures, we checked how they react to high-temperature gradient, and we interpreted the optical data in terms of growth conditions, In content, internal strain and In segregation.

2. Materials and methods

In this work, four samples were grown by molecular beam epitaxy (MBE) on an epi-ready GaAs(001) substrate. After oxide removal and outgassing at 615 °C for 5 min, a 200 nm-thick GaAs buffer was deposited at 570 °C. Then, the sample temperature was lowered to deposit the In(Ga)As nanostructures of interest, which were followed by 15 nm of GaAs grown at the same temperature and 85 nm of GaAs grown at 570 °C. Sample A contained conventional SKQDs obtained by depositing 2.2 MLs of InAs at 515 °C with a growth rate of 0.1 ML/s and an As_2 flux equivalent to 1.8 ML/s provided by a valved As cracker. Sample B contained InAs/GaAs SMLQDs grown under the same conditions as sample A, as usually done in the literature, but at 490 °C. Their structure consisted of six consecutive repetitions of 0.5 ML of InAs followed by 2.5 MLs of GaAs. The growth of these layers started on a c(4×4)-reconstructed GaAs(001) surface resulting from the usual conditions employed (high As_2 flux and low growth temperature). Sample C had the same structure as sample B, but the SMLQDs were deposited on a GaAs(001) surface with a (2×4) reconstruction which is supposed to provide a better formation of the 2D InAs islands than with the other reconstruction [19,20]. To maintain such a (2×4) reconstruction at low temperature—it is the usual GaAs(001) reconstruction above 525 °C—the As_2 flux had to be considerably lowered [21]. This, in turn, also required a strong reduction of the other fluxes to maintain an As-rich surface during growth [22]. As a consequence, the In, Ga, and As_2 fluxes were set to 0.015 ML/s, 0.1 ML/s, and 0.15 ML/s, respectively. Finally, sample D was a reference sample containing an $In_{0.17}Ga_{0.83}As$/GaAs quantum well (QW) having the same well thickness (5.1 nm) and average composition as the SMLQDs of samples B and C.

After growth, each sample was cleaved into two pieces: one was kept as grown, whereas the other was submitted to rapid thermal annealing before PL measurement. The RTA process occurred in a dedicated furnace in the presence of an N_2 atmosphere, and the samples were covered by another piece of GaAs to prevent As loss from their surface. The temperature was then abruptly raised to 900 °C, kept at that value for 30 s, and finally quickly reduced back to room temperature. The PL measurements were performed in an optical helium closed-cycle cryostat with a cold finger allowing the temperature to range between 10 and 300 K. The samples were excited by a solid-state laser emitting at 730 nm. The luminescence signal was dispersed and detected either by a 75 cm spectrometer and a Si-CCD (for the SMLQDs and QW) or by a 50 cm spectrometer and an InGaAs diode-array detector (for the SKQDs), depending on the spectral emission of the samples. In both cases, 150 l/mm diffraction gratings—blazed at 800 and 1250 nm, respectively—were used.

3. Results

Fig. 1 shows the low-temperature PL spectra of sample A (SKQDs) before and after RTA. Three main features can be observed:

before RTA, the spectrum is weaker, broader, and peaked at lower energy. These features are typical of SKQDs and were already reported earlier [18]. The lower intensity is related to the presence of structural defects in as-grown SKQDs that are formed by self-assembling, resulting in 4–7 nm high structures that need to be covered later by GaAs. Due to the lattice mismatch between InAs and GaAs, the capping process leads to the introduction of point defects at the interface between both materials [23,24]. The rapid thermal annealing promotes the diffusion of In atoms out of the SKQDs to relax the local strain and, simultaneously, contributes to reducing the number of defects, which act as non-radiative centers, producing an increase in the optical signal. This out-diffusion of In atoms leads to nanostructures with a lower In content and therefore to a material with a larger bandgap, which is responsible for the blueshift of the PL emission. This phenomenon is also responsible for the size homogenization of the QDs ensemble which manifests itself as a narrowing of the spectrum—the full width at half maximum (FWHM) went from 37.2 meV before RTA to 18.1 meV after RTA.

The PL spectra of sample B (before and after RTA), which contains SMLQDs deposited in conditions similar to those of sample A, are shown in Fig. 2. One can observe striking differences with respect to Fig. 1. Before RTA, the emission is much narrower (FWHM = 9.7 meV) and peaked at much higher energy than the as-grown SKQDs of Fig. 1. After RTA, not much happens: there is a very small blueshift of the emission, whose intensity slightly increased, and a slight reduction of the FWHM (to 8.6 meV) could be detected. The very narrow emission of SMLQDs has already been reported earlier [11] and is often associated, though erroneously, with a higher size homogeneity of SMLQDs. However, cross-sectional scanning tunneling microscopy (XSTM) measurements already pointed out that such nanostructures were very irregular and could not account for such narrow spectra. Instead, Harrison et al. [16] showed that this characteristic is due to the very small size of the nanostructures that provide effective confinement of holes but only very weak confinement of electrons. The wave function of electrons is consequently able to overlap the closest SMLQDs and their surroundings, leading to an average of the local composition fluctuations and, thus, to a narrow PL emission. The higher energy value of the peak is generally attributed to their smaller size but is mainly due to their lower In content resulting from the nominal InAs/GaAs periodic structure of the SMLQDs. The fact that the main optical properties of that sample do not change much after RTA can be explained as follows. The very small blueshift (around ten times smaller than in Fig. 1) is due to the much lower In content of these nanostructures (33% nominally in the present case instead of 55–85% in SKQDs [18]), which reduces the internal strain and, consequently, the out-diffusion of the In atoms during RTA. The slightly stronger PL signal after RTA is a sign that the density of defects in as-grown SMLQDs is much lower than in SKQDs. This is expected, as the submonolayer technique provides narrow 2D InAs islands that can be easily covered by GaAs to form the stacks. On the other hand, SKQDs are large 3D InAs islands that are much more difficult to be capped, resulting in the introduction of defects at their surface as a consequence of the lattice mismatch between both materials [23, 24]. The similar FWHM of the emissions before and after RTA is also a consequence of the low out-diffusion of In atoms which is not strong enough to change the composition and size distribution of these nanostructures in a relevant way.

Fig. 3 shows the PL data of sample C which contains SMLQDs having a structure identical to that of sample B but grown under different conditions to start with a (2×4) surface reconstruction rather than the c(4×4) reconstruction obtained with the common growth conditions of sample B. Previous STM studies already showed that 2D InAs islands could only be nucleated on the GaAs(001) surface when it was (2×4) reconstructed prior to the deposition [20]. On the contrary, the c(4×4) reconstruction obtained with the growth conditions used for SKQDs invariably lead to the random incorporation of the In atoms into the deep arsenic trenches of that surface, resulting in the formation of an InGaAs alloy instead of 2D InAs islands [19]. Therefore, one might expect in sample C the nucleation of true 2D InAs islands, providing then a better formation of the SMLQDs and a higher In content, which should somehow manifest themselves in the PL spectra. One can see in Fig. 3 that sample C exhibits the same features as sample B in Fig. 2—i.e., a narrow emission whose energy and width are only slightly affected by RTA (FWHM = 7.2 meV before RTA and FWHM = 7.3 meV after RTA)—suggesting that nothing very different happened, whatever the growth conditions. As a consequence, it seems reasonable to

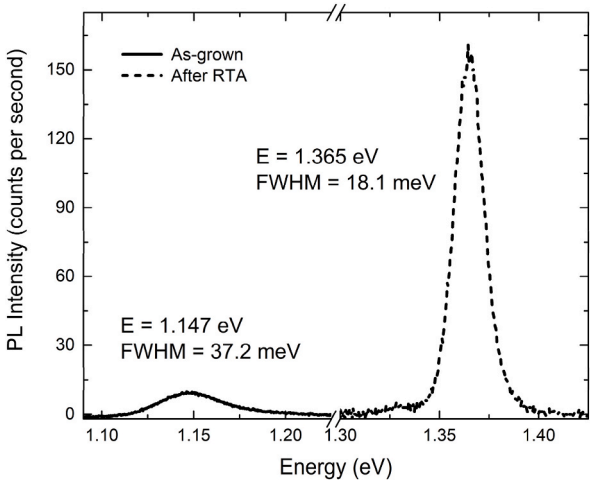

Fig. 1. PL spectra of sample A (SKQDs) before (full line) and after (dotted line) RTA. The measurements were performed at 10 K with an excitation power of 9.6 nW.

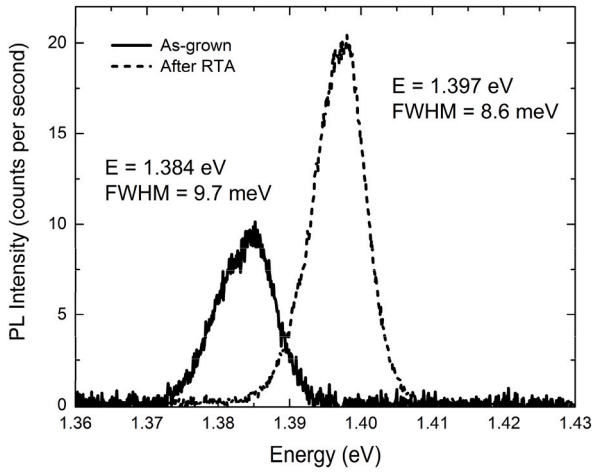

Fig. 2. PL spectra of sample B (SMLQDs with a c(4×4) surface reconstruction) before (full line) and after (dotted line) RTA. The measurements were performed at 10 K with an excitation power of 9.6 nW.

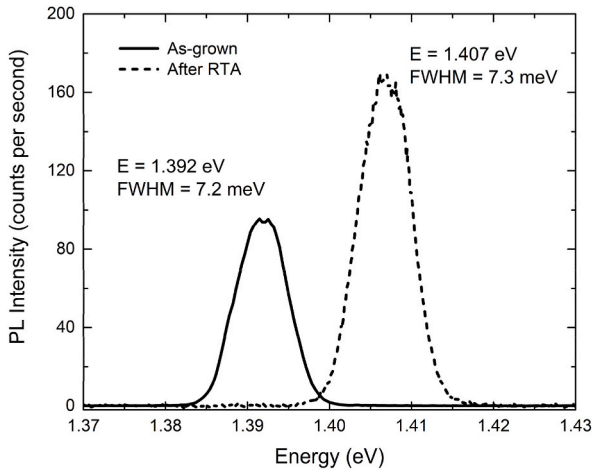

Fig. 3. PL spectra of sample C (SMLQDs with a (2×4) surface reconstruction) before (full line) and after (dotted line) RTA. The measurements were performed at 10 K with an excitation power of 9.6 nW.

suspect that some phenomenon currently limits the formation of good SMLQDs as will be discussed later.

Several works report that SMLQDs have optical properties very similar to those of an InGaAs quantum well [11,12,16], which may suggest that such nanostructures do not form or, eventually, could be optically inactive. From this point of view, sample D provides a reference for the present study, as its $In_{0.17}Ga_{0.63}As$ quantum well has the same nominal thickness (18 MLs) and average composition as samples B and C that contain SMLQDs. Fig. 4 confirms that sample D has indeed optical properties very similar to those of both SMLQDs samples before and after RTA, showing a narrower emission (FWHM = 7.2 meV before RTA and FWHM = 7.5 meV after RTA) peaked at higher energy and with a higher intensity than SKQDs. As a result, it might sound legitimate to believe that SMLQDs layers actually behave as an InGaAs quantum well. The tiny differences between the spectra of samples B, C, and D would thus originate from small fluctuations of the growth parameters or measurement conditions. However, this hypothesis can be easily ruled out as, when such SMLQDs are inserted in the active region of an infrared photodetector, the absorption signal under normal incidence is extremely strong [22,25], which would be impossible with quantum wells. Indeed, due to their 2D nature, polarization rules inhibit intraband transitions in quantum wells when the incident radiation reaches the surface perpendicularly, leading to very poor performance of quantum-well infrared photodetectors (QWIPs). This is why they always require a diffraction grating or another similar system to operate properly [26] in such conditions. As a consequence, although their optical properties may seem very similar, samples B and C must somehow contain zero-dimensional nanostructures that differentiate them from sample D.

Another relevant difference between SKQDs and SMLQDs comes from the dependence of their PL spectra on optical power. SKQDs usually show multiple emissions with increasing optical excitation, related to the presence of several confined electronic states (Fig. 5). On the other hand, SMLQDs always exhibit one single emission, even at the highest optical power, related to their ground state which is the only confined state (Fig. 6). These observations are compatible with PL experiments as a function of temperature: when the integral

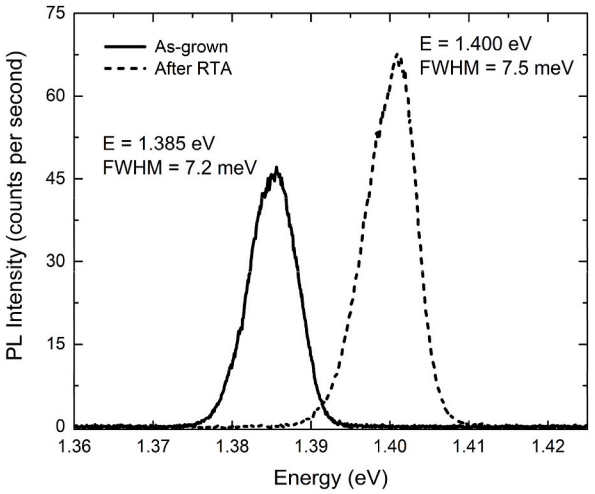

Fig. 4. PL spectra of sample D (quantum well) before (full line) and after (dotted line) RTA. The measurements were performed at 10 K with an excitation power of 9.6 nW.

of the ground-state emission is plotted as a function of the inverse of the absolute temperature (Arrhenius plot), one can easily obtain the activation energy E_a of the nanostructures under investigation by fitting the linear part of the graph (in a monolog plot) with the equation:

$$I = Ce^{-\frac{E_a}{k_B T}}, \tag{1}$$

where I is the integrated PL intensity, C is a constant of proportionality, k_B is the Boltzmann constant, and T is the absolute temperature. Before RTA, E_a was found to be 289 meV for sample A and between 99 and 118 meV for the other samples (Table 1 and Fig. 7). For usual InAs SKQDs, which have a large size and a high In content, a value of 60–70 meV is typically found between the energy levels of consecutive excited electronic states. With an activation energy of 289 meV, our SKQDs might therefore have four or five confined states. As quantum dots are known to exhibit a strong phonon bottleneck, one expects their PL spectra to reflect the presence of these states at high excitation power as can be seen in Fig. 5, where three of them are clearly observed. Since SMLQDs are smaller and have a lower In content, their ground-state energy is pushed up, their activation energy is naturally much smaller, and one expects the energy separation between possible consecutive confined states to be larger than 70 meV. Consequently, it seems reasonable that they can accommodate only the ground state, as seen in Fig. 6.

4. Discussion

It is clear from all these results that there are huge differences between SKQDs and SMLQDs, and that, from some points of view, the

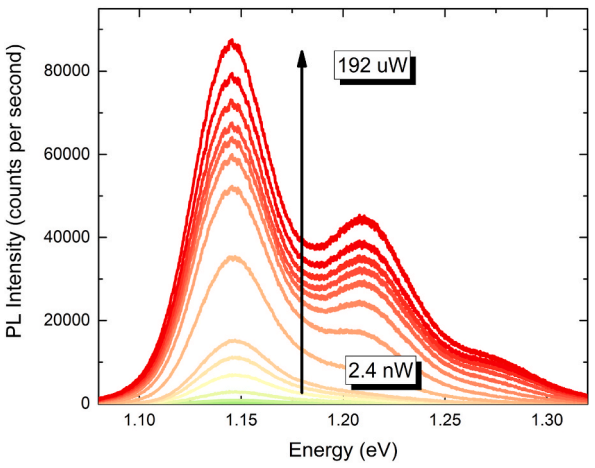

Fig. 5. PL spectra of sample A (SKQDs) before RTA as a function of the excitation power. After RTA, the spectra were alike, except that they were blueshifted and narrower, as already pointed out in Fig. 1. The measurements were performed at 10 K.

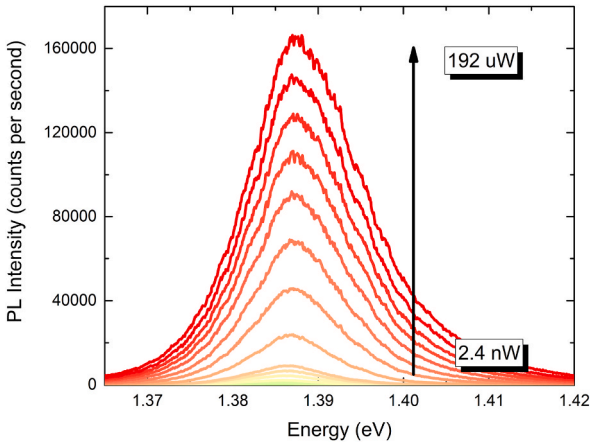

Fig. 6. PL spectra of sample B (SMLQDs with a c(4×4) surface reconstruction) before RTA as a function of the excitation power. Samples C and D had a very similar dependence, as well as the pieces that underwent the RTA process. The measurements were performed at 10 K.

Table 1
Activation energies and respective uncertainties extracted from the Arrhenius plots (Fig. 7). The "difference" column shows the activation energy after RTA minus the activation energy before RTA.

Sample	Nanostructure	Activation energy (meV)		
		As-grown	After RTA	Difference
A	SKQD	289 (7)	150 (1)	−139 (7)
B	SMLQD c(4×4)	99 (1)	73.9 (9)	−25 (1)
C	SMLQD (2×4)	107 (2)	88 (1)	−19 (2)
D	QW	118.4 (8)	125 (1)	7 (1)

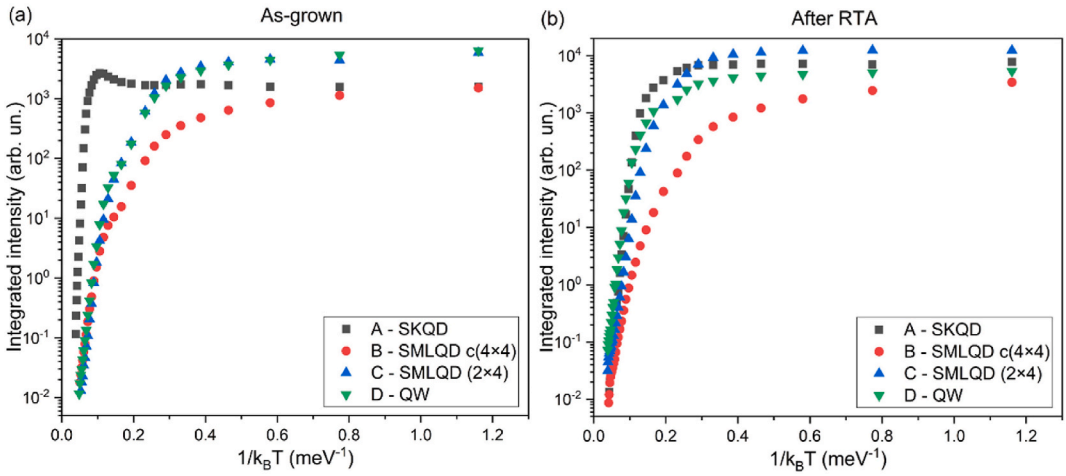

Fig. 7. Arrhenius plots of all the samples (a) before and (b) after RTA. The measurements were performed with an excitation power of 19.2 μW. The activation energies were extracted from the linear region of the plots (left side, corresponding to higher temperatures) and are presented in Table 1.

latter seems to behave as quantum wells. However, it is also undeniable that the use of SMLQDs in several types of devices already provided much progress when compared to SKQDs or QWs, which confirms their high value and potential. As a consequence, it is clearly necessary to further investigate these nanostructures and identify what phenomenon may limit their properties to eventually come out with solutions and continue improving their performance.

Recent XSTM measurements showed that SMLQDs are generally shorter than expected—they do not develop their full nominal height—and usually show no periodic internal structure related to the vertical stacking of small 2D InAs islands. Instead, irregular InGaAs clusters are observed inside a thicker InGaAs layer having a lower In content [16,17]. This was attributed to the strong segregation of In atoms that is always present in the InAs/GaAs system, where segregation coefficients *R* around 0.8 are often measured

[11,27–31]. The very high value of this coefficient means that 80% of the In atoms present at the surface of the sample or originating from the In cell migrate with the growth front and will only be incorporated later. This, of course, seriously hinders the formation and vertical alignment of the 2D InAs islands, whose material is spread in the next layers—not necessarily inside the SMLQDs themselves—and contributes to forming the InGaAs layer with a lower In content that surrounds the SMLQDs.

This strong segregation effect is most probably responsible for the extremely weak influence of RTA over the main features of the PL spectra of the SMLQDs samples. The main consequence is that the nominal structure of samples B and C, consisting of stacks of small 2D InAs islands surrounded by GaAs material, is replaced by In-rich clusters dispersed in a dilute InGaAs quantum well. Therefore, the actual In content of the nanostructures relative to the surrounding matrix is much lower than expected, providing SMLQDs with smaller strain. In such conditions, when the samples undergo the RTA process, there is only a very weak diffusion of the In atoms out of the quantum dots which barely affects their optical properties, as can be seen in Figs. 2 and 3. This is confirmed in Fig. 4 where sample D, which is a normal InGaAs QW containing no QDs of any type, shows the same kind of changes after RTA.

The assumption that small 2D islands from consecutive InAs submonolayers should stack to form SMLQDs originates from previous observations of vertical alignment of SKQDs in consecutive InAs layers when their separation was smaller than tens of nanometers [32]. One expects the same to occur in SMLQDs due to the strain field created by the lattice mismatch between the 2D InAs islands and the GaAs material around them. However, since segregation acts to partially dissolve the original 2D InAs islands—reducing the In content of the nanostructures and increasing the In content of the surrounding matrix—one might wonder whether the internal strain field is still strong enough to produce an effective alignment of these 2D islands.

Xie et al. [32] developed a semiempirical model able to evaluate the strain field around InAs SKQDs embedded in a GaAs matrix and its ability to influence the nucleation of SKQDs in the next InAs layer close by. They found out that SKQDs of consecutive InAs layers were always vertically aligned whenever the GaAs spacer was thinner than a certain value z_0, which mainly depends on the size of the SKQDs, their average lateral separation, the lattice parameters of InAs and GaAs, as well as several elastic constants of both materials. They calculated that typical SKQDs should stack vertically with a probability larger than 95% whenever their vertical separation was smaller than 10 nm and should be completely uncoupled for distances larger than 50 nm, in excellent agreement with their experimental observations.

Because of the very thin GaAs spacer existing between consecutive InAs submonolayers, one expects such a vertical alignment of the 2D InAs islands to occur as well to form SMLQDs. This is why these nanostructures are invariably sketched as stacks of 2D InAs islands separated by thin layers of GaAs material. However, one should be aware of several relevant differences between SMLQDs and SKQDs. First of all, SMLQDs are much smaller and have a larger areal density. In addition, the influence of In segregation is much stronger in SMLQDs, which actually consist of tiny 3D In-rich InGaAs clusters dispersed in a thick InGaAs matrix. It means that the lattice parameters and elastic constants of both materials are much closer than for InAs SKQDs separated by thick GaAs layers. Altogether, these changes lead to a drastic reduction of the internal strain field and of z_0 that might reach values below 2 MLs [33]. Although the model of Xie et al. was developed for small spherical QDs and may not provide accurate results for the 2D islands forming the SMLQDs, it is clear from all XSTM results so far that the lack of vertical alignment is most probably related to the very low value of z_0 that should then be smaller than 2 MLs.

With these differences between SMLQDs and SKQDs in mind, it is now easier to understand the experimental results presented above. Due to the self-assembling process that reshapes the original InAs layer into large 3D islands, buried SKQDs contain a high quantity of In (up to 85%) [18] and are surrounded by a GaAs matrix which leaves them under considerable strain. Their large size and high In content provide a much deeper ground state—resulting in large activation energy—and allow the existence of several excited states that can be probed at higher optical power (Fig. 5). During RTA, there is a strong out-diffusion of In atoms that considerably modifies their optical properties: the size of the nanostructures increases and their In content is reduced (down to 36%) [18], yielding a wider bandgap and a blueshift of all the energy levels. In the case of SMLQDs, the situation is quite different. Due to the strong segregation of In atoms during the formation of the nanostructures themselves, their In content—which is already nominally much lower (33%) than in SKQDs—is further reduced because of the detachment of many In atoms from the 2D islands. This In material is mostly scattered in the surrounding matrix that is now made of InGaAs instead of GaAs. From XSTM images, one can roughly estimate that the SMLQDs contain around 20% of In, and the surrounding matrix has about half of that [17]. In such conditions, the real SMLQDs are very different from the nominal ones and are under much lower stress than SKQDs. When they go through the RTA process, the diffusion of In atoms out of the SMLQDs is much weaker because their In content is close to that of the surrounding InGaAs layer, resulting in only very small changes of their structural and optical properties. It seems that the only physical parameter that allows to differentiate them from the $In_{0.17}Ga_{0.83}As$ quantum well of sample D is their activation energy—even their dependences of the integrated intensity on excitation power are similar (for more details, see the supplementary material). The activation energies of samples B and C (SMLQDs) were reduced by 25% and 17% after RTA, respectively, while the activation energy of sample D was barely affected and actually increased by 6%. For the SKQDs, a reduction of 48% was observed—resulting from their higher In content and stronger influence of the RTA process.

Finally, let us compare samples B and C. Although they have the same nominal structure, samples B and C were grown in very different conditions but showed similar optical properties, the exception being the intensity of their PL emission, which is an order of magnitude higher in sample C ((2×4) surface reconstruction). Harrison et al. [16] showed, by means of eight-band k•p calculations, that the electron spatial localization in InAs/GaAs SMLQDs improves when the difference in concentration between the In-rich InGaAs agglomerates and the surrounding InGaAs matrix increases. Furthermore, XSTM results [17] revealed that the (2×4) surface reconstruction leads to a much lower In concentration in the surrounding matrix compared to the c(4×4) surface reconstruction, mainly because of the reduced incorporation of In atoms in the presence of the very low As_2 flux required to stabilize that specific surface reconstruction. Therefore, it is likely that electrons have a higher degree of spatial localization in sample C than in sample B, which

should improve the overlap between the electron and hole wave functions and, consequently, also the PL intensity of that sample.

From a practical point of view, the overall similarities between the optical properties of samples B and C are already a positive result, as it means that growth conditions do not affect much the formation of SMLQDs. In this case, the very easy growth conditions of sample B—which are similar to those of SKQDs—should be preferred as they also result in shorter growth times [22]. However, these conditions were not supposed to form small 2D InAs islands [19]. Even so, they somehow enabled a high density of In rich agglomerates that behaved as zero-dimensional nanostructures, as already confirmed by the high performance of SML-QDIPs [34]. On the other hand, sample C was obtained with very different conditions (more difficult to reach) that should favor the formation of 2D InAs islands and provide more robust SMLQDs. Its slightly higher PL energy probably comes from the smaller size of the quantum dots and from their lower In content resulting from reduced incorporation of In atoms in the presence of the weak As_2 flux necessary to stabilize the (2×4) surface reconstruction [17,27]. XSTM data showed that the nanostructures of sample C also consisted of small InGaAs clusters without any periodicity related to the vertical alignment of 2D InAs islands. However, despite their lower areal density—when compared to SMLQDs obtained with a c(4×4) surface reconstruction—they performed very well in QDIPs as well [22,33]. These similar properties are once again a consequence of the strong segregation effect that destroys most 2D InAs islands of sample C and scatters their material around, allowing it to incorporate randomly later. There is thus the formation of small and irregular In-rich InGaAs clusters dispersed in a thick InGaAs matrix that make samples B and C look alike and have properties similar to those of the InGaAs quantum well of sample D. As a consequence, In segregation seems definitely to be the main obstacle to overcome to get SMLQDs of better quality [34]. A higher concentration of In inside these 2D islands would strengthen the strain field necessary to align them and form In-richer structures that could finally provide stronger three-dimensional confinement of the carriers. As segregation is thermally activated, a natural way to control it would be to reduce the growth temperature. However, lower temperatures also contribute to worsening the crystalline quality of the epitaxial layers [35], and it will thus be necessary to find a compromise. Only in this way will it be worth using the more difficult growth conditions of sample C to get better devices.

5. Conclusions

Four samples with the same structure but containing different InGaAs/GaAs nanostructures have been grown by molecular beam epitaxy: one containing InAs Stranski-Krastanov quantum dots (sample A), two with InAs/GaAs submonolayer quantum dots deposited in the presence of a c(4×4) (sample B) and (2×4) (sample C) surface reconstruction, and the last one consisting of an InGaAs quantum well with the same thickness and average composition as in samples B and C. Before rapid thermal annealing, sample A had a broad emission peaked at low energy, while the other three samples had a much narrower emission peaked at higher energy. After rapid thermal annealing, the spectrum of sample A became narrower, much more intense, and blueshifted when compared to the as-grown sample, while the optical properties of the other three samples remained similar to the original ones. The strong modifications observed in sample A originate from the large size and high In content of Stranski-Krastanov quantum dots that suffer a strong out-diffusion of In atoms resulting from their high internal strain. On the other hand, due to their nominal structure, submonolayer quantum dots have naturally a lower In content that is reduced further by the presence of strong segregation that scatters a large part of the In atoms in the thin GaAs interlayers. The main consequence is that the internal strain is no longer strong enough to promote a vertical alignment of the two-dimensional InAs islands that are supposed to be the building blocks of these nanostructures. This is why submonolayer quantum dots usually look like irregular In-rich InGaAs agglomerates scattered in a dilute InGaAs matrix. As a result, it seems that In segregation needs to be controlled if one wants to keep improving the properties of such nanostructures.

Credit authors statement

T. F. Cantalice: Investigation, Validation, Formal analysis, Writing – original draft. A. Alzeidan: Investigation, Resources, Visualization. G. M. Jacobsen: Investigation, Validation, Formal analysis, Data curation. T. Borrely: Validation, Formal analysis, Writing – review & editing. M. D. Teodoro: Resources, Supervision, Funding acquisition, Writing – review & editing. A. A. Quivy: Conceptualization, Methodology, Resources, Supervision, Funding acquisition, Project administration, Writing – review & editing.

Declaration of competing interest

The authors declare that they have no known competing financial interests or personal relationships that could have appeared to influence the work reported in this paper.

Data availability

Data will be made available on request.

Acknowledgments

This study was financed in part by the Coordenação de Aperfeiçoamento de Pessoal de Nível Superior - Brasil (CAPES) - Finance Code 001 and by Conselho Nacional de Desenvolvimento Científico e Tecnológico (CNPq) (grant 311687/2017-2). The authors also acknowledge the financial support of the Fundação de Amparo à Pesquisa do Estado de São Paulo (FAPESP)—grants 2018/06328-1 and 2014/19142-2.

Appendix A. Supplementary data

Supplementary data to this article can be found online at https://doi.org/10.1016/j.micrna.2022.207449.

References

[1] Q. Xie, A. Kalburge, P. Chen, A. Madhukar, Observation of lasing from vertically self-organized InAs three-dimensional island quantum boxes on GaAs (001), IEEE Photon. Technol. Lett. 8 (1996) 965–967, https://doi.org/10.1109/68.508705.

[2] Z. Chen, O. Baklenov, E.T. Kim, I. Mukhametzhanov, J. Tie, A. Madhukar, Normal incidence InAs/AlxGa1−xAsInAs/AlxGa1−xAs quantum dot infrared photodetectors with undoped active region, J. Appl. Phys. 89 (2001) 4558–4563, https://doi.org/10.1063/1.1356430.

[3] N. López, A. Marti, A. Luque, C. Stanley, C. Farmer, P. Diaz, Experimental analysis of the operation of quantum dot intermediate band solar cells, J. Sol. Energy Eng. 129 (2007) 319–322, https://doi.org/10.1115/1.2735344.

[4] D. Leonard, M. Krishnamurthy, C.M. Reaves, S.P. Denbaars, P.M. Petroff, Direct formation of quantum sized dots from uniform coherent islands of InGaAs on GaAs surfaces, Appl. Phys. Lett. 63 (1993) 3203–3205, https://doi.org/10.1063/1.110199.

[5] T. Asano, A. Madhukar, K. Mahalingam, G.J. Brown, Dark current and band profiles in low defect density thick multilayered GaAs/InAs self-assembled quantum dot structures for infrared detectors, J. Appl. Phys. 104 (2008), 113115-5, https://doi.org/10.1063/1.3039799.

[6] A. Martí, N. López, E. Antolín, E. Cánovas, A. Luque, C.R. Stanley, C.D. Farmer, P. Díaz, Emitter degradation in quantum dot intermediate band solar cells, Appl. Phys. Lett. 90 (2007) 233510–233513, https://doi.org/10.1063/1.2747195.

[7] A.V. Barve, S. Sengupta, J.O. Kim, Y.D. Sharma, S. Adhikary, T.J. Rotter, S.J. Lee, Y.H. Kim, S. Krishna, Confinement enhancing barriers for high performance quantum dots-in-a-well infrared detectors, Appl. Phys. Lett. 99 (2011) 191110–191113, https://doi.org/10.1063/1.3660317.

[8] X.H. Su, J. Yang, P. Bhattacharya, G. Ariyawansa, A.G.U. Perera, Terahertz detection with tunneling quantum dot intersublevel photodetector, Appl. Phys. Lett. 89 (2006), 031117-3, https://doi.org/10.1063/1.2233808.

[9] S. Krishna, Quantum dots-in-a-well infrared photodetectors, J. Phys. D Appl. Phys. 38 (2005) 2142–2150, https://doi.org/10.1088/0022-3727/38/13/010.

[10] I.L. Krestnikov, N.N. Ledentsov, A. Hoffmann, D. Bimberg, Arrays of two-dimensional islands formed by submonolayer insertions: growth, properties, devices, Phys. Status Solidi A 183 (2001) 207–233, https://doi.org/10.1002/1521-396X(200102)183:2%3C207::AID-PSSA207%3E3.0.CO.

[11] A. Lenz, H. Eisele, J. Becker, J.H. Schulze, T.D. Germann, F. Luckert, K. Pötschke, E. Lenz, L. Ivanova, A. Strittmatter, D. Bimberg, U.W. Pohl, M. Dähne, Atomic structure and optical properties of InAs submonolayer depositions in GaAs, J. Vac. Sci. Technol. B 29 (2011), 4D104-8, https://doi.org/10.1116/1.3602470.

[12] L. Yu, D. Jung, S. Law, J. Shen, J.J. Cha, M.L. Lee, D. Wasserman, Controlling quantum dot energies using submonolayer bandstructure engineering, Appl. Phys. Lett. 105 (2014) 81103–81105, https://doi.org/10.1063/1.4893983.

[13] H. Ghadi, S. Sengupta, S. Shetty, A. Manohar, A. Balgarkashi, S. Chakrabarti, N.B. Pendyala, S.L. Prajapati, A. Kumar, Comparison of three design architectures for quantum dot infrared photodetectors: InGaAscapped dots, dots-in-a-well, and submonolayer quantum dots, IEEE Nanotechnol 14 (2015) 603–607, https://doi.org/10.1109/TNANO.2015.2432044.

[14] P. Lam, J. Wu, M. Tang, Q. Jiang, S. Hatch, R. Beanland, J. Wilson, R. Allison, H. Liu, Submonolayer InGaAs/GaAs quantum dot solar cells, Sol. Energy Mater. Sol. Cells 126 (2014) 83–87, https://doi.org/10.1016/j.solmat.2014.03.046.

[15] T.D. Germann, A. Strittmatter, J. Pohl, U.W. Pohl, D. Bimberg, J. Rautiainen, M. Guina, O.G. Okhotnikov, High-power semiconductor disk laser based on InAs/GaAs submonolayer quantum dots, Appl. Phys. Lett. 92 (2008), 101123-3, https://doi.org/10.1063/1.2898165.

[16] S. Harrison, M.P. Young, P.D. Hodgson, R.J. Young, M. Hayne, L. Danos, A. Schliwa, A. Strittmatter, A. Lenz, H. Eisele, U.W. Pohl, D. Bimberg, Heterodimensional charge-carrier confinement in stacked submonolayer InAs in GaAs, Phys. Rev. B 93 (2016) 85302–85309, https://doi.org/10.1103/PhysRevB.93.085302.

[17] R.S.R. Gajjela, A.L. Hendriks, A. Alzeidan, T.F. Cantalice, A.A. Quivy, P.M. Koenraad, Cross-sectional scanning tunneling microscopy of InAs/GaAs(001) submonolayer quantum dots, Phys. Rev. Materials. 11 (2020) 114601–114607, https://doi.org/10.1103/PhysRevMaterials.4.114601.

[18] J.G. Keizer, A.B. Henriques, A.D.B. Maia, A.A. Quivy, P.M. Koenraad, Atomically resolved study of the morphology change of InAs/GaAs quantum dot layers induced by rapid thermal annealing, Appl. Phys. Lett. 101 (2012) 243113–243114, https://doi.org/10.1063/1.4770371.

[19] J.G. Belk, C.F. McConville, J.L. Sudijono, T.S. Jones, B.A. Joyce, Surface alloying at InAs/GaAs interfaces grown on (001) surfaces by molecular beam epitaxy, Surf. Sci. 387 (1997) 213–226, https://doi.org/10.1016/S0039-6028(97)00355-5.

[20] G.R. Bell, T.J. Krzyzewski, P.B. Joyce, T.S. Jones, Island size scaling for submonolayer growth of InAs on GaAs(001)-(2x4): strain and surface reconstruction effects, Phys. Rev. B 61 (2000) 10551–10554, https://doi.org/10.1103/PhysRevB.61.R10551.

[21] V.P. LaBella, M.R. Krause, Z. Ding, P.M. Thibado, Arsenic-rich GaAs(001) surface structure, Surf. Sci. Rep. 60 (2005) 1–53, https://doi.org/10.1016/j.surfrep.2005.10.001.

[22] A. Alzeidan, M.S. Claro, A.A. Quivy, High-detectivity infrared photodetector based on InAs submonolayer quantum dots grown on GaAs(001) with a 2×4 surface reconstruction, J. Appl. Phys. 126 (2019), 224506-6, https://doi.org/10.1063/1.5125238.

[23] M.M. Sobolev, I.V. Kochnev, V.M. Lantratov, N.A. Bert, N.A. Cherkashin, N.N. Ledentsov, D.A. Bedarev, Thermal annealing of defects in InGaAs/GaAs heterostructures with three-dimensional islands, Semiconductors 34 (2000) 195–204, https://doi.org/10.1134/1.1187932.

[24] N.A. Hastas, C.A. Dimitriadis, L. Dozsa, E. Gombia, R. Mosca, Investigation of single electron traps induced by InAs quantum dots embedded in GaAs layer using the low-frequency noise technique, J. Appl. Phys. 96 (2004) 5735–5739, https://doi.org/10.1063/1.1801163.

[25] J.O. Kim, Z. Ku, A. Kazemi, A. Urbas, S.W. Kang, S.K. Noh, S.J. Lee, S. Krishna, Effect of barrier on the performance of submonolayer quantum dot infrared photodetectors, Opt. Mater. Express 4 (2014) 198–204, https://doi.org/10.1364/OME.4.000198.

[26] B.F. Levine, Quantum well infrared photodetectors, J. Appl. Phys. 74 (1993) R1–R18, https://doi.org/10.1063/1.354252.

[27] K. Muraki, S. Fukatsu, Y. Shiraki, R. Ito, Surface segregation of in atoms during molecular beam epitaxy and its influence on the energy levels in InGaAs/GaAs quantum wells, Appl. Phys. Lett. 61 (1992) 557–559, https://doi.org/10.1063/1.107835.

[28] S. Martini, A.A. Quivy, E.C.F. Silva, J.R. Leite, Real-time determination of the segregation strength of indium atoms in InGaAs layers grown by molecular-beam epitaxy, Appl. Phys. Lett. 81 (2002) 2863–2865, https://doi.org/10.1063/1.1513182.

[29] S. Martini, A.A. Quivy, T.E. Lamas, M.J. Silva, E.C.F. Silva, J.R. Leite, Influence of indium segregation on the RHEED oscillations during the growth of InGaAs layers on a GaAs(001) surface, J. Cryst. Growth 251 (2003) 101–105, https://doi.org/10.1016/S0022-0248(02)02313-8.

[30] S. Martini, A.A. Quivy, T.E. Lamas, E.C.F. Silva, Real-time RHEED investigation of indium segregation in InGaAs layers grown on vicinal GaAs(001) substrates, Phys. Rev. B 72 (2005), 153304-4, https://doi.org/10.1103/PhysRevB.72.153304.

[31] S. Martini, A.A. Quivy, M.J. Silva, T.E. Lamas, E.C.F. Silva, J.R. Leite, E. Abramof, Ex-situ investigation of indium segregation in InGaAs/GaAs quantum wells using high resolution x-ray diffraction, J. Appl. Phys. 94 (2003) 7050–7052, https://doi.org/10.1063/1.1621738.

[32] Q. Xie, A. Madhukar, P. Chen, N.P. Kobayashi, Vertically self-organized InAs quantum box islands on GaAs(100), Phys. Rev. Lett. 75 (1995) 2542–2545, https://doi.org/10.1103/PhysRevLett.75.2542.

[33] A. Alzeidan, T.F. Cantalice, K.D. Vallejo, R.S. R Gajjela, A.L. Hendriks, P.J. Simmonds, P.M. Koenraad, A.A. Quivy, Effect of as flux on InAs submonolayer quantum dot formation for infrared photodetectors, Sens. Actuators, A 334 (2022), 113357, https://doi.org/10.1016/j.sna.2021.113357.
[34] T.F. Cantalice, A. Alzeidan, S. Urahata, A.A. Quivy, In-situ measurement of indium segregation in InAs/GaAs submonolayer quantum dots, Mater. Res. Express 6 (2019) 126205–126210, https://doi.org/10.1088/2053-1591/ab55a8.
[35] S. Fleischer, C.D. Beling, S. Fung, W.R. Nieveen, J.E. Squire, J.Q. Zheng, M. Missous, Structural and defect characterization of GaAs and AlxGa1−xAs grown at low temperature by molecular beam epitaxy, J. Appl. Phys. 81 (1997) 190–198, https://doi.org/10.1063/1.364105.